Microwave Synthesis of Zeolites: 1. Reactor Engineering

Wm. Curtis Conner* and Geoffrey Tompsett

Department of Chemical Engineering, University of Massachusetts, Amherst, Massachusetts 01003

Kyo-Ho Lee and K. Sigfrid Yngvesson

Department of Electrical and Computer Engineering, University of Massachusetts, Amherst, Massachusetts 01003

Received: November 4, 2003; In Final Form: May 17, 2004

Studies in the past decade suggest that microwave energy may have a unique ability to influence chemical processes. These include chemical and materials syntheses as well as separations. Specifically, recent studies have documented significantly reduced time for the fabrication of zeolites employing microwave energy. However, the mechanism and engineering for the enhanced rates of syntheses are unknown. The results from different laboratories are not consistent, and experimental details are sparse. We studied the synthesis of silicalite employing two geometries in an oven with 2.45-GHz microwaves. The distribution of microwave energies within the reactors from simulation differed, and the morphologies and yields of the resultant zeolite also differed. Larger uniform silicalite crystals were formed in the larger reactor in which the variation in microwave energy distribution was greater. Engineering the energy distribution within a microwave synthesis reactor is necessary to understand and control the process.

Background

Microwave energy has been employed in many recent chemical reaction studies and has been found to change the kinetics and selectivity, often in favorable ways. These reactions include organic and inorganic syntheses, selective sorption, oxidations/reductions, and polymerizations, among many other processes.[1] Microwave energy is found to be more efficient in the selective heating in many processes. The most recent American Chemical Society monograph on green chemistry[2] recommends for us to "Use methods that minimize the energy required for a reaction to take place. For example... catalysts or microwave radiation".

One of the most exciting (and commercially/technologically significant) areas where microwave energy has been demonstrated to influence the kinetics and selectivity is the synthesis of nanoporous materials. New nanoporous materials can be created, and the times for their syntheses can be significantly reduced, involving less energy. By reducing the times by up to over an order of magnitude, continuous production would be possible to replace batch synthesis. Recent studies have demonstrated this in laboratory experiments with[3] and without[4] microwaves. Additional microwave syntheses have proved to create more uniform systems (defect free) than conventional hydrothermal synthesis procedures.

We studied two zeolite synthesis reactor geometries. The products were characterized by infrared FTIR, X-ray diffraction (XRD), and scanning electron microscopy (SEM). The silicalite products differed in their morphology. We analyzed the distribution of microwave energy present in the two reaction reactors by simulation, and the energy distribution was also found to differ significantly. This combination of experimental and simulation demonstrates that microwave energy can influence the sequence of steps giving rise to the rapid synthesis of zeolites in several ways. The reactor engineering must be considered in order to understand and control microwave synthesis.

Zeolite Synthesis

The first patent for the microwave synthesis of zeolites was issued in 1988 to Mobil for the synthesis of zeolites NaA and ZSM-5.[5] The patent claims the "ability to provide relatively small crystals at higher rates of productivity". The microwave syntheses of over a dozen zeolites have been disclosed and studied in a score of laboratories over the past decade.[6] These are briefly summarized in Table 1. In each case, the studies demonstrate that microwave syntheses take considerably less time than conventional hydrothermal techniques, to well over an order of magnitude shorter (e.g., 10 min for microwave versus 10−50 h for conventional hydrothermal syntheses of NaY[7] or 2 h versus 14 days for the synthesis of MCM[8−11]). However, there are considerable differences in the claims from different laboratories. Zhao et al. claim the synthesis of Y-zeolite in 20 min,[12] Arafat et al. claim 40 min,[7] Katsuki et al.[13] claim 1−3 h, and Slangen et al.[14] claim 4 h, all at similar temperatures. Similar inconsistencies are found between laboratories for other studies of similar zeolites. Some of the reasons for these discrepancies are discussed below. In each case, these laboratories demonstrate that similar synthesis mixtures take an order of magnitude more time with conventional heating. Each laboratory conducted their synthesis in microwave ovens often using temperature control of the synthesis mixtures and 2.45-GHz radiation.

Microwave energy has also been found to be advantageous in the synthesis of many substituted zeolites[10,25−27] and other nanoporous molecular sieves,[28−30] incorporating metals within or on the surface of the high-surface-area solids.

* To whom correspondence should be addressed. E-mail: wconner@ecs.umass.edu.

10.1021/jp037358c CCC: $27.50
Published on Web 07/09/2004

TABLE 1: Survey[a] of the Microwave Synthesis of Nanoporous Materials

zeolite type	microwave hydrothermal treatment − power, time, temperature	characterization
silicalite membrane	180 °C, 15 min, with 10 min induction at 85 °C[15]	
Na-A powder	120 °C, 90 s → 100 °C, 10 min;[16] 100 °C, 5 min, 0.1−0.3 μ, 1 min, 300 W[17]	XRD
Na-A membrane	250 W, 10 min shows A-type crystals in gel 12 min[18]	XRD
	500-nm crystals after 15 min,[19] 15 min at 90 °C [20]	
Na-Y powder	300 W, 2 h, 180−280-μ crystal size, 96% yield[13]	XRD
	14 h at 170 °C[12]	XRD
Na-Y(EMT) powders	1.5 h at 110 °C[12]	XRD
Y-zeolite powder	30 s, 120 °C then 10 min at 100 °C[7]	XRD
cubic Y powder	900 W at 120 °C in 30 s, 18−25 min at 120 °C [21]	XRD and FTIR
analcium powder	1000 W up to 1200 min[22]	XRD and FTIR
Na-P1 powder	1000 W, up to 1200 min[22]	XRD and FTIR
Ti-ZSM-5 powder	950 W max[12]	XRD
Beta- powder	14 h at 140°C[12]	XRD
ZSM-5 powder	160 °C 1 min, 30 min at 140 °C[7,23,24]	XRD and FTIR
[Al]ZSM-5 powder	5 min at 175 °C with seeding, 2.5 h at 175 °C	XRD
	without seeding;[24] 7 + 1.5 h at 170 °C[12]	

[a] Abbreviated.

The proposed mechanisms for the synthesis of nanoporous crystalline oxides from solution involve a sequence of steps.[31] It is perceived that an amorphous gel is formed from solution by the association of the hydroxides or other dissolved reagents. Ringlike structures form from the gel, creating microcrystalline domains (<1 nm) that are the precursors of the unit cells of the porous crystals. The unit cells (primary building blocks) then nucleate to form small single crystals (~10 nm) of the nanoporous crystalline product. These single crystals then grow in dimension (to $>10^5$ nm) by reaction at their surface. This can involve the incorporation of reagents from solution, including microcrystalline domains. Mechanisms such as Ostwald ripening (the redissolution of molecules or domains from single crystals already formed react to grow other crystals) can also contribute to this final growth process.

Exposure to microwave energy may influence each of these processes. It could enhance the rate of gel formation as well as the rate of formation of microcrystalline domains, of the nucleation of single crystals, and/or of the growth of single crystals to the final product. It might independently (or in combination) influence the molecular processes leading to these steps in the formation of nanoporous solids. These include the condensation of MOH (M′−O−H) species to form M−O−M or M−O−M′ bonds (M = metal atom) within the resultant solid metal oxide. The reactant species are dissolved within the precursor solution, forming various associations with solvating species (e.g., water). Microwave energy has been proposed to perturb these interactions and to enhance the rate of formation of M−O−M′ bonds. Each of these influences has been proposed to explain the unique syntheses in the presence of microwave energy.

We have studied silicalite formation from tetraethyl orthosilicate with a template (tetrapropylammonium hydroxide, TPOAH) as an example. The basic reaction is described by the following equations: (1) the formation of silicon hydroxide and (2) the condensation of silicon hydroxide to form SiO_2 solid (with template TPA forming silicate rings).

$$Si(C_2H_5O)_4 + 4H_2O \rightarrow Si(OH)_4 + 4C_2H_5OH \qquad (1)$$

$$Si(OH)_4 + [TPA] \rightarrow SiO_2(s)[TPA](s) + 2H_2O \qquad (2)$$

Several hypotheses have been advanced to explain the enhancement in the synthesis rate for zeolites:

(I) Microwave energy increases the heating rate of the synthesis mixture, increasing the rate.[13]

(II) Microwave energy leads to a more uniform heating of the synthesis mixture.[32]

(III) Microwaves change the association between species within the synthesis mixture.[33,34]

(IV) Microwave heating superheats the synthesis mixture.[35]

(V) Hot spots are created within the synthesis mixture.[16,24]

(VI) Microwave energy enhances the dissolution of the precursor gel.[34,36,37]

These hypotheses are reviewed and discussed by Cundy.[6] In addition, we suggest that specific reactions might be enhanced in a microwave field or by the absorption of microwave energy by reactants, intermediate species, and/or products.

Reactor Engineering

Microwave reactors are not necessarily isothermal. This fact will influence the performance of these reactors in chemical processes. The distribution of energy can be manipulated by a variety of factors including the reactor geometry, delivery system, and frequency. There is little question that species in solution leading to the synthesis of structured oxides differ in their absorption of microwave energy. Does this varying absorption give rise to variations in temperature within the reacting mixture, or is heat convection/conduction fast enough to make the system isothermal?

Prior studies of microwave energy in inorganic synthesis or chemistry have most often employed a microwave oven, such as that used in your kitchen. Essentially all have used 2.45-GHz excitation. Small amounts of material, typically 50−100 cm^3, are contained in glass or Teflon reactors placed in the oven. In isothermal experiments, the temperature is controlled by employing a fiber optic probe. Typically, the 2.45-GHz power is turned on and off as the measured temperature is below or above that desired. In a few cases, the reactor is placed in a rotating carousel to average its exposure.

There are several inconsistencies between these prior experiments. These include the field homogeneity, power delivery, and reactor geometry. Few of these complexities are discussed or specified in any prior studies. Dielectric resonance could produce maxima and nulls in the microwave fields throughout the samples. Stenzel et al.[32] designed an applicator for the microwave heating of aqueous solutions for the hydrothermal synthesis of zeolites. The electric and thermal design was optimized by numerical simulations of the E field and of the temperature distribution. Different temperature profiles could be created by simply altering the dimensions of the applicator.

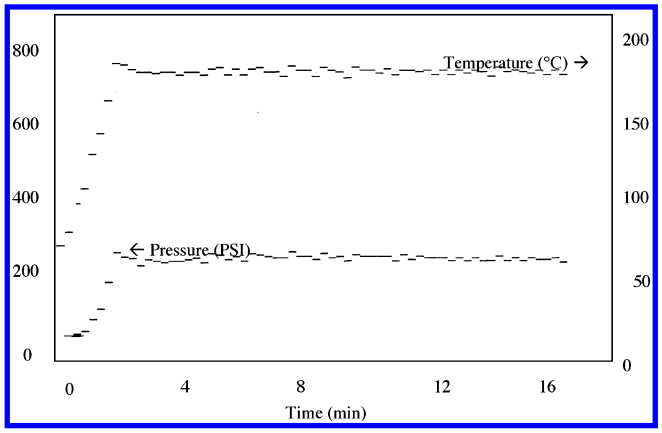

Figure 1. Temperature and pressure profile of silicalite solution in a MARS5 microwave while heating to 175 °C for 15 min with a 2-min ramp time and a 600-W power maximum for the 33-mm-diameter reactor.

They proposed that the more uniformly heated reactor was desirable for synthesizing zeolites A and VPI-5 and designed their applicator accordingly.[32]

Bonaccorsi and Proverbio[38] investigated the influence of the reactor geometry on the penetration depth of the microwaves on the zeolite synthesis. Two spherical reactors were used of volumes 100 and 500 mL , into each of which 50 g of the reaction mixture was placed. This gave two surface-to-volume ratios of 0.67 and 1.45 mm^{-1}, respectively. The reactor with a higher surface-to-volume ratio gave low crystallization and a higher level of impurities for the synthesis of the NaA zeolite. This was attributed to the low penetration depth, which results in energy build up in the external surface of the mixture, resulting in the formation of amorphous structures.

We demonstrate that engineering the energy distribution within a microwave synthesis reactor is necessary to understand and control the process.

Experimental Section

Silicalite Syntheses Solutions. Silicalite solutions were prepared on the basis of known procedures.[39] Synthesis solutions were prepared by mixing 25 g of tetraethylorthosilicate (TEOS, Aldrich 98%), 26.25 g of tetrapropylammonium hydroxide (TPAOH, Aldrich; a 1 M solution in water), and 48.75 g of H_2O with stirring for 4 h at room temperature. The same volume (10 mL) was then measured into the microwave reactors using a volumetric flask. The pH of the reaction solutions was measured at room temperature before and after microwave heating.

Microwave Synthesis. A MARS5 (CEM Corporation) microwave laboratory oven was used with a 1200-W maximum at 2.45 GHz. The internal dimensions of the microwave cavity are 420 (w) × 340 (d) × 330 (h) mm^3. The MARS5 oven has a single magnetron that operates using continuous power up to 100% of the set maximum power of either 300, 600, or 1200 W. Under "ramp to temperature" mode, the power is automatically adjusted in a continuous field to achieve the ramp time and temperature selected. The temperature was monitored with a fiber optic probe inside a Teflon-coated glass thermowell in the center of the reaction vessel. The vessel pressure was also monitored using a shielded pressure transducer clamped above the reaction vessel. Figure 1a shows a typical plot of temperature and pressure for a 33-mm-i.d. vessel heated to 175 °C in 2 min and held for 15 min before cooling. The temperature and pressure measurements are scaled images of each other, reflecting the vapor−liquid equilibria for the synthesis solution (i.e., $P(T)_{VLE}$). There is no evidence of superheating for the bulk solution or discrepancies between measurements of T and P.

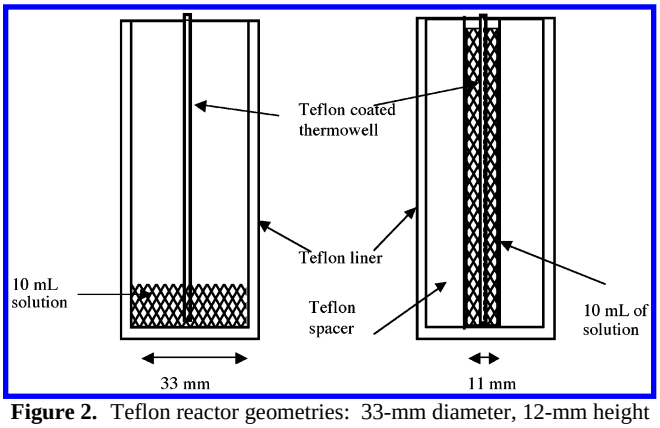

Figure 2. Teflon reactor geometries: 33-mm diameter, 12-mm height and 11-mm diameter, 105-mm height.

The vessels consist of 100-mL Teflon liners inside glass fiber insulation sleeves. The vessel is capped with a stretched lid and is held in a polypropylene holder. Four vessels in holders (one reaction vessel and three empty vessels) were used within the microwave cavity to balance the rotating carousal. The reaction vessels lock into a carousal that rotates 360° clockwise then counterclockwise every 4−5 s.

Two vessels with different inside diameters were employed to determine the effect of reaction vessel geometry on the synthesis product. Figure 2 shows a schematic of the reaction vessels. Microwave heating was carried out using 600-W maximum power, a 2-min ramp time (with maximum of 100% power), and a specific (but variable) hold time at 175 °C. On completion of the heating hold step, the microwaves were stopped, and the solution was allowed to cool to room temperature before removal. Multiple samples were run in both reactor sizes with cleaning between runs.

The same volume and composition of synthesis solution was added to each reactor. The surface-to-volume (S/V) ratios for the two reactors were 0.38 mm^{-1} for the 11-mm-diameter reactor and 0.26 mm^{-1} for the 33-mm-diameter reactor. This gives a difference of ∼1.5× in the S/V ratios between the two reaction volumes investigated.

Synthesis suspension solutions were cloudy, indicating the formation of a solid in suspension. The solid product was retrieved using repeated ultracentrifuging at >100 000 rpm and washing with distilled water. The solid powder was then dried overnight at 90 °C. Average yields were determined from the dry weight of solids from the 11- and 33-mm-diameter reactors of 1 and 45%, respectively, for 15 min of reaction.

Characterization. The products were characterized by three standard techniques: FTIR, XRD, and scanning electron microscopy (SEM). The dielectric properties of the reactants and products were also measured by microwave spectroscopy.

Mid-infrared spectra of the zeolite powders were obtained using a Bruker Equinox 5 FTIR spectrometer. A resolution of 4 cm^{-1} and averaging of 50 scans were used for the spectra. Samples were prepared as KBr pellets of 12.5-mm diameter using approximately a 1 wt % sample with respect to KBr.

Powder X-ray diffraction of the dried silicalite from microwave synthesis was carried out using a Philips X'Pert X-ray diffractometer. X-ray patterns were excited using a Cu Kα X-ray source. A scanning rate of 0.02°(2θ)/s was used at 45-kV and 40-A power settings.

High-resolution electron micrographs of the dried silicalite powders were obtained using a Joel JSM-5400 scanning electron

TABLE 2: Dielectric Constants of Silicalite and Precursor Chemicals Measured with an HP 8510C Network Analyzer and an HP 85070B Dielectric Probe

component	literature dielectric constant, ϵ	reference	dielectric permittivity ϵ' (2.45 GHz, 25 °C)[a]	dielectric loss ϵ'' (2.45 GHz, 25 °C)[a]
tetraethyl-ortho-silicate (TEOS) (98%)	4.1 (20 °C)	41	4.10	0
ethanol	24.3 (25 °C)	41	7.85	7.09
water	80.4 (20 °C)	41	78	10.33
TPAOH (1 M solution)			47.64	86.24
silicalite powder	1.6	42	1.83	0.06
precursor solution (25 g TEOS 98%, 26.25 g TPAOH 1 M, and 48.75 g H_2O)			49.54	20.13
Teflon (PTFE) reactor	2	41		

[a] This work.

microscope. A 15-keV electron source was used, and resolved images were captured at 10 000× magnification.

The complex permittivity and loss tangent of silicalite were measured from 0.5 to 17 GHz using an HP 8510C Network Analyzer and an HP 85070B dielectric probe kit (Hewlett-Packard).

Analyses. The ability of microwave energy to transfer energy to a material depends on its permittivity. We measured the actual susceptibility of the reaction solution to 2.45-GHz microwave energy (i.e., its complex permittivity) and simulated the distribution of microwave energy within the different reactors employed in these studies.

The permittivity of a material reflects its dielectric absorptivity and is often expressed as a complex expression with a real part ϵ', reflecting the field-induced charge separation, and an imaginary part ϵ'', reflecting the absorbed energy that is converted into heat. There is a strong dependence of permittivity on the frequency for the measurement of these permittivities in our starting synthesis solution and final product suspension. The typical microwave frequency used in domestic and laboratory microwave ovens is 2.45 GHz.

The permittivity of the material is important in simulating the field concentration and heating of the material. Water has a very high dielectric constant $\epsilon' = 80$ at 20 °C. The conductivity and hence dielectric properties of the synthesis solution will vary from that of distilled water because of the presence of the zeolite and precursor ions in suspensions (e.g., the pH). As the zeolite is formed in suspension, the dielectric constant might change. The dielectric constants reported in the literature (not at 2.45 GHz) for silicalite, the precursor components and solution are listed in Table 2. The measured dielectric permittivity and loss at 2.45 GHz are also listed in Table 2. These have an estimated accuracy of ±5% (HP specs.) but are less accurate for smaller permittivity values (e.g., silicalite) because of noise. Pure methanol and deionized water were employed as standards.

The dielectric permittivity of the solution dictates the penetration depth, δ, at which the microwave field has decayed by $^1/_e$ of its intensity. For water, we find that $\delta = 3$ cm up to a pH of 12.5, whereas $\delta = 0.7$ cm for pH 13.5. In the typical zeolite suspensions used by Stenzel et al.,[32] they estimated that $\delta =$ 0.3 to 0.5 cm. However, this was obtained with suspensions of zeolites A and VPI-5 in water and did not take into account the pH of the solution or the presence of other precursor or product species.

The permittivity variation with temperature is complicated and is dependent on the thermal conductivity of the material.[40] Stenzel et al.[32] measured the dielectric properties of different zeolite suspensions as a function of temperature and found that under typical synthesis conditions $\epsilon' \approx 40$ and $\epsilon'' = 20-160$.

We simulated the electric field distribution in the two reactors to determine the potential effect on the reaction kinetics. Agilent HFSS (High Frequency Structure Simulator, version 5.6) software has been used to simulate the E-field distribution in different column diameters in a microwave cavity. The software initially produces 3D meshes within 3D volumes. The program refines the mesh in order to optimize the field distribution. Maxwell's equations are solved automatically within the created meshes[43] with the appropriate boundary conditions.

We used the following parameters to obtain the most realistic approximation of the field distribution in the reactors. The actual oven dimensions were used for the simulated cavity at 420 (w) × 340 (d) × 330 (h) mm^3. The complex permittivity and loss tangent of silicalite were measured using an HP 8510C network analyzer and HP 85070B dielectric probe kit (Hewlett-Packard). The measured real and imaginary parts of the relative permittivity and loss of silicalite solutions at pH 12.28 and 2.45 GHz are shown in Table 2. The room-temperature (298 K) measurements were used for the solutions reaction because the permittivity and loss factor show only a small (<20%) increase during reaction and we have yet to develop the in situ permittivity measurements. The 2.45-GHz microwave generator is attached to the oven by a waveguide of the same dimensions as employed in the MARS5. The waveguide is attached to the center of one side of the oven. The cylindrical reactor is positioned in the center of the oven on the bottom surface, just as in the actual oven. An input power of 1 W was employed in the simulations.[43] We have also determined that the cavity size, generator position, and reactor position all contribute significantly to the electric field distribution, and this will be discussed in a later publication.[44] However, the chosen generator position and reactor closely approximate the real situation in the microwave oven and provide a simulation that demonstrates the difference in the E-field distribution in the two reactors.

Results and Discussion

Silicalite was synthesized using a MARS5 (CEM) microwave oven. Identical synthesis solutions were reacted under the same conditions of time, temperature, and heating rate employing two different reactor geometries, namely, cylindrical 11- and 33-mm-diameter reactors. The synthesized crystals were retrieved using centrifugation, washing, and drying. Figure 3 shows the SEM micrographs of the dried crystals from the two reactors with different geometry. The crystals produced from the wider-diameter reactor have a larger and more uniform microstructure after 15 min at 175 °C (Figure 3). They exhibit a *c*-axis dimension (longest face) of >2 μm of the classic "coffin" shape, whereas the crystals from the 11-mm-diameter reactor are <1 μm with a more circular (spherical) shape. The larger reactor produced more numerous, larger crystals, whereas the smaller reactor produced fewer, smaller, spherical crystals (i.e., the morphologies differ; see Table 3). From the average particle

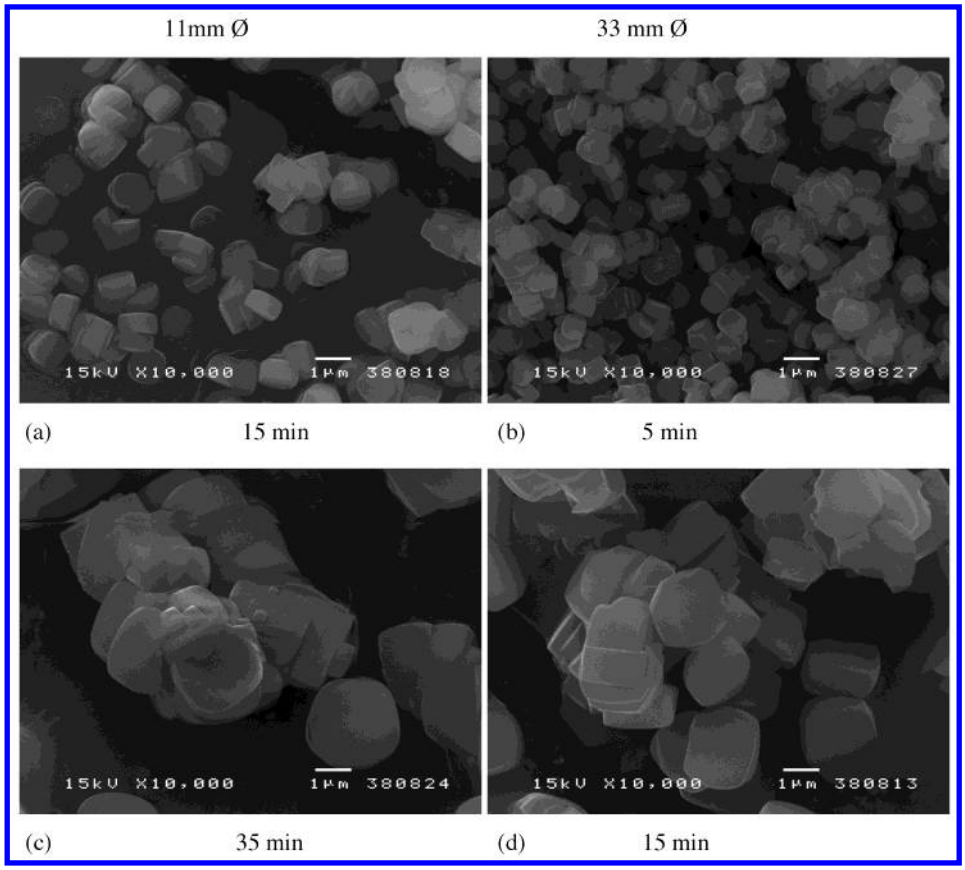

Figure 3. SEM micrographs (10 000× magnification) of silicalite from microwave synthesis: (a) 15 min, 175 °C, 11-mm-diameter reactor, (b) 5 min, 175 °C, 33-mm-diameter reactor, (c) 35 min, 175 °C, 11-mm-diameter reactor, and (d) 15 min, 175 °C, 33-mm-diameter reactor. (Scale bar indicates 1 μm).

TABLE 3: Yield, pH, Permittivity, Loss, Measurements for Silicalite Synthesis Solutions, and the Relative Number and Sizes for the Product Silicalite Particles

synthesis time at 175 °C	reactor diameter (mm)	yield (wt %)	pH after	dielectric permittivity (ϵ') (±5%) at 2.45 GHz	dielectric loss (ϵ'') (±5%) at 2.45 GHz	relative number of particles	crystal size $c \times a$ axis (μm)
precursor solution			12.28	49.5	20.2		
5 min	33	3	12.5	53.6	20.7	100	$c = 0.75 \pm 0.04$ $a = 0.65 \pm 0.04$
15 min	33	45	12.53	54.5	21.9	56	$c = 2.1 \pm 0.1$ $a = 1.72 \pm 0.09$
15 min	11	1	12.28	56.4	21.2	9.8	$c = 1.03 \pm 0.05$ $a = 0.98 \pm 0.08$
35 min	11	6	12.17	55.3	21.8	4.3	$c = 2.4 \pm 0.1$ $a = 2.1 \pm 0.2$

size and yields, we estimate that the larger-diameter reactor produced 5 times more crystals than the smaller-diameter reactor in 15 min.

Silicalite crystals were synthesized for different time periods at 175 °C using the two reactors. The synthesis solution was reacted for different periods of time to show the morphology and crystal size as the reaction proceeds in the two reactors. As shown in Figure 3a and c, the crystal morphology for the 11-mm reactor exhibits a more circular shape. After 15 min, the crystal size (longest axis) was only ca. 1 μm compared to >2 μm observed for the crystals in the 33-mm reactor reacted for the same time and temperature. After 35 min of reaction time in the 11-mm-diameter reactor, the crystals have grown to >2 μm; however, the shape has remained more circular compared to the classical elongated hexagonal coffin observed from the 33-mm-diameter reactor. After only 5 min using the 33-mm-diameter reactor, the crystals are ca. 0.5 μm in length and exhibit the coffin shape with no twins. The crystal morphology is determined early on in the reaction and continues with crystal growth in time at the same temperature.

The yields, pH, and dielectric permittivity were measured for each type of preparation method; the results are shown in Table 3. The permittivity and loss values of the suspensions after reaction at 175 °C for both reactors show little change at 2.45 GHz; however, the permittivity increases slightly. Similarly, the pH after reaction shows a slight increase over that of the precursor. The yields are markedly different for the reactors, the smaller-diameter reactor giving consistently lower yields (over an order of magnitude lower) even after extended reaction times (35 min). The sample dimensions were estimated from the SEM micrographs by sampling 96 random particles and performing statistical analysis of the measured sizes. As a representative sample from the large ($\sim 10^{12}$) population of crystals, this gives a 95% confidence level, at a <10% margin of error, using statistical standard sample-size estimates.[45] The number of particles produced was then estimated from the

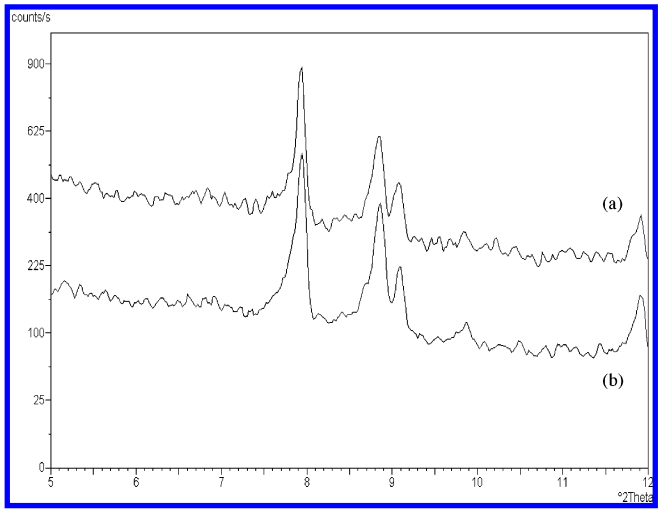

Figure 4. XRD patterns of silicalite prepared by microwave hydrothermal 175 °C, 600 W, for 15 min in (a) an 11-mm-diameter reactor and (b) a 33-mm-diameter reactor.

measured yields and particle dimensions, again within 10%. The number of particles produced in the 33-mm reactor after 5 min was arbitrarily assigned as 100, and the others were expressed relative to this. These data represent an average of 5+ runs for each set of conditions with <5% variation between runs. As the particle sizes increase, the number apparently decreases in each reactor, and the sizes are smaller and an order of magnitude less numerous in the smaller reactor.

Figure 4 shows the X-ray diffraction patterns for silicalite powders produced from two different geometries. It can be seen that the same XRD pattern is observed for both samples. In each case, the pattern was identical to that observed for conventional-growth silicalite crystals. There was no evidence of other crystalline phases formed. The infrared spectra were obtained for the same silicalite powders, as shown in Figure 5. The same spectrum is obtained for both samples from microwave synthesis in the two different geometry reactors. Bands at 450, 550, 800, 1100, and 1225 cm^{-1} match those reported for silicalite.[46] This is consistent with X-ray diffraction data and confirms that a single-phase silicalite material is produced. The main difference is the crystal morphology, as shown in Figure 3.

It is important to understand the microwave field distribution within the reactor to interpret the influence of reactor configuration on microwave-synthesized crystal morphology. Simulation software was employed to provide a picture of the electric and magnetic field distributions in the different reactors. This technique was successfully demonstrated by Stenzel et al.[32] using HFSS software.

We also used Agilent HFSS software to study the effect of the differing reactor geometries (solution column shape) on the electric field distribution. Figure 6 shows the 3D graph of the electric field distribution in both the 11- and 33-mm-diameter solution columns placed in a 420 (w) × 340 (d) × 330 (h) mm^3 cavity with a microwave frequency of 2.45 GHz. The "up" dimension reflects the microwave power density at various points in the 2D plane through the center of each reactor. The power density is color scaled blue = cold → red = hot, as seen in the bar on the right side of each graph. These are instantaneous snapshots of the local energy. The measured dielectric parameters of the silicalite prepared solution $\epsilon' = 49.5$, $\epsilon'' = 20.15$, and $\tan \delta = 0.407$ were used in this calculation.

Several features can be determined from the graphs. Namely, the 11-mm column shows a single mode with an even field

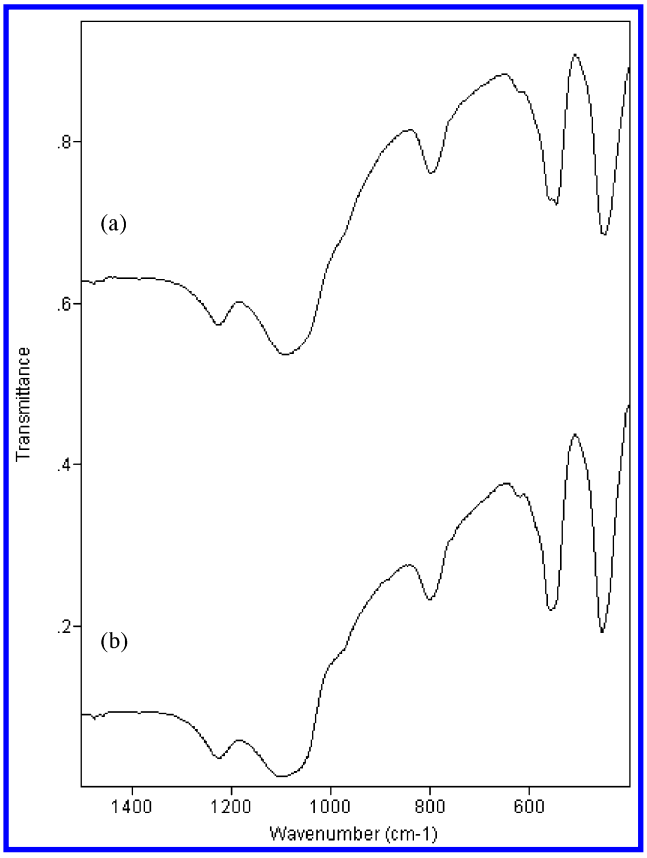

Figure 5. FTIR spectra of silicalite prepared by microwave hydrothermal 175 °C, 600 W, for 15 min in (a) an 11-mm-diameter reactor and (b) a 33-mm-diameter reactor.

distribution, and the 33-mm column has a multimode distribution. The ratio of maxima to minima energy is also greater for the 33-mm-diameter column than for the the 11-mm-diameter column: 2.43 compared to 1.34. Therefore, the variation in energy within the 33-mm reactor is approximately twice that observed for the 11-mm reactor, and the field distribution indicates the presence of multiple "hot spots", in this case, concentric high-energy regions. With reference to the crystal morphology produced in the larger reactor, these hot spots apparently give rise to increased growth over nucleation. This might be due to an enhanced Ostwald ripening in a reactor with regions of high intensity promoting the redissolution of the crystals in that region that then diffuse to the less intense regions where particles continue to grow. There is apparently less crystal growth in the smaller reactor and less nucleation because the yield is significantly lower. The multimode distribution and the lower surface-to-volume ratio for the liquid in the 33-mm reactor influence the kinetics of the synthesis reaction and, thus, the product yield and morphology.

It should be noted that the distributions of energy shown in Figure 6 could not be achieved by conventional heating of a sample. Indeed, only microwave energy (at 2.45 GHz) could create these distributions of high and low energy intensity (i.e., local heating seen in Figure 6). The result is a unique combination of relative reaction rates giving rise to a morphologically different product. However, even the more uniform heating of the synthesis mixture by microwave energy in the smaller reactor results in a significant increase in the rate compared to that of hydrothermal synthesis, so there may be more to rate enhancement by microwaves than just the creation of hot spots.

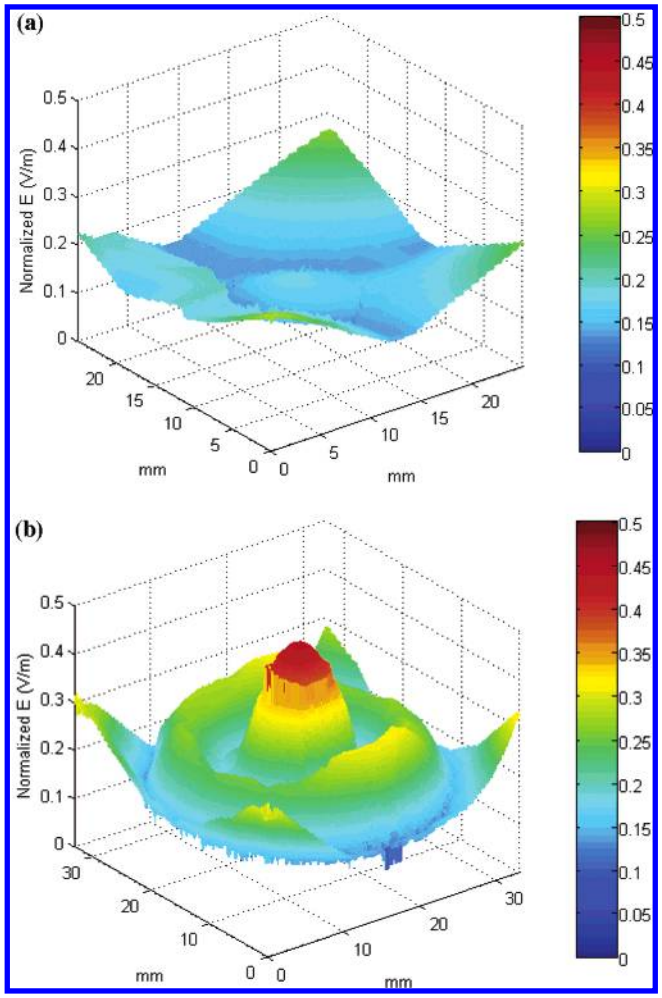

Figure 6. HFSS simulation of the electric field distribution in (a) an 11- and (b) a 33-mm-diameter column. The microwave power density is shown in the vertical direction and is scaled to the color bar on the right side. The cross section through the center of each column is shown into the plane of the paper. The following simulation was employed: 10 mL of silicalite solution at 298 K, resonant cavity size 109.22 (w) × 54.61 (h) × 73.9 (l) mm^3, 2.45 GHz, $\epsilon' = 49.5$, $\epsilon'' = 20.15$, tan $\delta = 0.407$, electric field normalized to 1000 V/m.

These studies demonstrate that the distribution of microwave energy within the reactor can vary depending on several factors, including the reactor geometry, dielectric permittivity, temperature, and frequency. Unless these factors are specified, results from different laboratories can appear inconsistent. (See above.) The resultant energy distribution can influence the relative rates of the processes involved in synthesis reactions and thus can control the final product (i.e., its morphology and yield). At another frequency, the resonant pattern and thus the distribution of energy as well as the kinetics will differ. The potential influence of microwave frequency on sorption and synthesis has yet to be discussed but is the subject of our continuing studies. We find that the influence of microwave energy on sorption can exhibit microwave effects that are consistent with similar selective heating at catalytic and adsorbent surfaces.[42]

Conclusions

The synthesis of silicalite employing two different reactor geometries in a laboratory microwave oven with 2.45-GHz microwaves was studied. Greater crystal growth was observed for the reactor geometry with 3 times the radius of the other, namely, 33- compared to 11-mm diameter. HFSS software was used to simulate the electric field distributions within these silicalite synthesis reactors within the microwave oven we used for the synthesis. The simulated distribution of microwave energies within the reactors differed (i.e., the larger reactor showed a multimode distribution with higher field maxima compared to that for the smaller 11-mm-diameter reactor). These multimode hot spots apparently give rise to the greater silicalite crystal growth and morphology observed. However, both microwave energy distributions induced zeolite synthesis in more than an order of magnitude less time than for hydrothermal synthesis at similar temperatures.

The synthesis of zeolites and other solids from solution involves a complex sequence of steps of varying kinetics and sensitivity to temperature. For isothermal hydrothermal synthesis, there is an optimum temperature for the growth of product of a desired morphology. Cundy has reviewed the potential influence of microwave energy on the chemical processes taking place and concludes that several thermal effects can explain the differences.[6] We concur but also show in this study that microwave energy can provide a nonuniform distribution of energy within a reactor and can efficiently, selectively, and rapidly heat the system. This variation of energy input within a reactor can sometimes significantly enhance the overall kinetics for a complex reaction network/sequence. With respect to the possible reasons for enhanced zeolite synthesis by microwaves (I−VI, above), we conclude that rapid heating (I) and the creation of hot spots (V) contribute to increases in silicalite synthesis rates. However, we are not suggesting that the same would be true for all zeolite syntheses, so we require more studies to determine the influence of microwaves on the enhancement of specific mechanistic steps (III or VI). There will be other situations (e.g., the synthesis of other zeolites) when nonuniform heating may be less beneficial or even may slow the rate of a reaction. A combination of experiment, simulation, and theory[47] are needed to understand and to take advantage of the potential for microwave energy to enhance synthesis, catalysis, and sorption. We are developing several in situ techniques to provide a direct view of the specific influence of microwave energy on synthesis, sorption, and catalysis involving solid oxides (e.g., zeolites).

This is a microwave effect that is due to a selective distribution of microwave fields and the resultant heating; however, this is not necessarily an *athermal* effect of microwave energy. Knowledge concerning the energy distribution gives considerable insight into the rates and mechanisms by which microwave energy enhances synthesis. Microwave reactor engineering will enable us fully to take advantage of the use of microwave energy in chemical synthesis, sorption, and catalysis.

Acknowledgment. We thank DuPont (L. Manzer and L. Abrams) for the support and discussion that initiated this project. Additional support was provided by the NSF under grant CTS 0002157 (Maria Burka) and NIRT grant CT-0304217 (Glenn Schrader) for this project. Also, G.T. and W.C. thank Dr. D. Sommerfeld, Department of Chemistry, University of Massachusetts, for the use of the microwave oven.

References and Notes

(1) Kingston, H. M. In *Microwave-Enhanced Chemistry*; Haswell, S. J., Ed.; American Chemical Society: Washington, DC, 1997.

(2) Matlack, A. S. *Introduction to Green Chemistry*; Marcel Dekker: New York, 2001.

(3) Braun, I.; Schulz-Ekloff, G.; Wohrle, D.; Lautenschlager, W. *Micropor. Mesopor. Mater.* **1998**, *23*, 79.

(4) Slangen, P. M.; Jansen, J. C.; van Bekkum, H.; Hofland, G. W.; van der Ham, F.; Witkamp, G. J. Continuous synthesis of zeolites using a tubular reactor; *Proceedings of the 12th International Conference on Zeolites*; Materials Research Society: Baltimore, 1999; Vol. 3, p 1553.
(5) Chu P, D.; Vartuli, F. G. U.S. Patent 4,778,666, 1988.
(6) Cundy, C. S. *Collect. Czech. Chem. Commun.* **1998**, *63*, 1699.
(7) Arafat, A.; Jansen, J. C.; Ebaid, A. R.; van Bekkum, H. *Zeolites* **1993**, *13*, 162.
(8) Park, S. E.; Kim, D. S.; Chang, J. S.; Kim, W. Y. *Catal. Today* **1998**, *44*, 301.
(9) Newalkar, B. L.; Komarneni, S.; Katsuki, H. *Phys. Chem. Chem. Phys.* **2000**, *2*, 2389.
(10) Kang, K. K.; Park, C. H.; Ahn, W. S. *Catal. Lett.* **1999**, *59*, 45.
(11) Wu, C. G.; Bein, T. *Chem. Commun.* **1996**, 925.
(12) Zhao, J. P.; Cundy, C.; Dwyer, J. Synthesis of Zeolites in a Microwave Heating Environment. In *Progress in Zeolite and Microporous Materials*, parts A−C, 1997; Vol. 105, p 181.
(13) Katsuki, H.; Furuta, S.; Komarneni, S. *J. Porous Mater.* **2001**, *8*, 5.
(14) Slangen, P. M.; Jansen, J. C.; van Bekkum, H. *Zeolites* **1997**, *18*, 63.
(15) Koegler, J. H.; Arafat, A.; van Bekkum, H.; Jansen, J. C. Synthesis of Films of Oriented Silicalite-1 Crystals Using Microwave Heating. In *Progress in Zeolite and Microporous Materials*, Pts A−C, 1997; Vol. 105, p 2163.
(16) Slangen, P. M.; Jansen, J. C.; van Bekkum, H. *Microporous Mater.* **1997**, *9*, 259.
(17) Pilter, Z.; Szabo, S.; Hasznos-Nezdei, M.; Pallai-Varsanyi, E. *Microporous Mesoporous Mater.* **2000**, *40*, 257.
(18) Han, Y.; Ma, H.; Qui, S. L.; Xiao, F. S. *Microporous Mesoporous Mater.* **1999**, *30*, 321.
(19) Xu, X. C.; Yang, W. S.; Liu, J.; Lin, L. W. *Chin. Sci. Bull.* **2000**, *45*, 1179.
(20) Xu, X. C.; Yang, W. S.; Liu, J.; Lin, L. W. *Adv. Mater.* **2000**, *12*, 195.
(21) de Araujo, L. R. G.; Cavalcante Jr, C. L.; Farias, K. M.; Guedes, I.; Sasaki, J. M.; Freire, P. T. C.; Melo, F. E. A.; Mendes-Filho, J. *Mater. Res.* **1999**, *2*, 105.
(22) Sathupunya, M.; Gulari, E.; Wongkasemjit, S. *J. Eur. Ceram. Soc.* **2002**, *22*, 2305.
(23) Kooyman, P. J.; vanderWaal, P.; vanBekkum, H. *Zeolites* **1997**, *18*, 50.
(24) Zhao, J. P.; Cundy, C. S.; Plaisted, R. J.; Dwyer, J. *Proc. Int. Zeolite Conf.* **1999**, 1591.
(25) Deng, S. G.; Lin, Y. S. *Chem. Eng. Sci.* **1997**, *52*, 1563.
(26) Wang, Y.; Zhu, J. H.; Cao, J. M.; Chun, Y.; Xu, Q. H. *Microporous Mesoporous Mater.* **1998**, *26*, 175.
(27) Xiao, F. S.; Qiu, S. L.; Pang, W. Q.; Xu, R. R. *Adv. Mater.* **1999**, *11*, 1091.
(28) Newalkar, B. L.; Olanrewaju, J.; Komarneni, S. *J. Phys. Chem. B* **2001**, *105*, 8356.
(29) Newalkar, B. L.; Olanrewaju, J.; Komarneni, S. *Chem. Mater.* **2001**, *13*, 552.
(30) Belhekar, A.; Agashe, M.; Soni, H.; Sathaye, S.; Jacob, N.; Thundimadathil, J. *Bull. Chem. Soc. Jpn.* **2000**, *73*, 2605.
(31) Serrano, D. P.; van Grieken, R. *J. Mater. Chem.* **2001**, *11*, 2391.
(32) Stenzel, C. B. M.; Müller, J.; Schertlen, R.; Venot, Y.; Wiesbeck, W. A. *Microwave Power Electro. Energy* **2001**, *36*, 155.
(33) Uguina M. A.; Serrano, D. P.; Sanz, R.; Castillo, E. *Proceedings of the 12th International Conference on Zeolites*; Materials Research Society: Baltimore, 1999; Vol. 3, p 1917.
(34) Girnus, I.; Jancke, K.; Vetter, R.; Richtermendau, J.; Caro, J. *Zeolites* **1995**, *15*, 33.
(35) Scharf, O. H., R, Schwieger, W. *Deutsche Zeolith-Tagung* **2002**, *6−8*.
(36) Xu, X. H.; Yang, W. H.; Liu, J.; Lin, L. W. *Sep. Purif. Technol.* **2001**, *25*, 241.
(37) Jansen, J. C.; Arafat, A.; Vanbekkum, H. *Abstr. Pap. Am. Chem. Soc.* **1991**, *202*, 80.
(38) Bonaccorsi, L.; Proverbio, E. *J. Cryst. Growth* **2003**, *247*, 555.
(39) Xomeritakis, G.; Nair, S.; Tsapatsis, M. *Microporous Mesoporous Mater.* **2000**, *38*, 61.
(40) Ayappa, K. A.; Davis, H. T.; Davis, E. A.; Gordon, J. *AIChE J.* **1991**, *37*, 313.
(41) ASI Instruments, Inc. http://www.asiinstr.com/dc1.html. 2003.
(42) Turner, M. D.; Laurence, R. L.; Conner, W. C.; Yngvesson, K. S. *AIChE J.* **2000**, *46*, 758.
(43) *HFSS Online Manual*; Agilent. http://eesof.tm.agilent.com/docs/hfss/tutorial/hfss56_tut.pdf. 2003.
(44) Lee, K. S.; Yngvesson, K. S.; Tompsett, G. A.; Conner, W. C. To be submitted for publication.
(45) Questair; http://www.questaresearch.com/calc_ss_std.php.
(46) Miecznikowski, A.; Hanuza, J. *Zeolites* **1987**, *7*, 249.
(47) Blanco, C.; Auerbach, S. M. *J. Phys. Chem. B* **2003**, *107*, 2490.